Virial coefficients of model alkanes

Andrew J. Schultz[a] and David A. Kofke[b]
Department of Chemical and Biological Engineering, University at Buffalo, The State University of New York, Buffalo, New York 14260-4200, USA

(Received 7 April 2010; accepted 13 August 2010; published online 8 September 2010)

We report the results from Mayer-sampling Monte Carlo calculations of the virial coefficients of the united-atom TraPPE-UA model of normal alkanes. For alkane chain lengths from $n=2$ to 20 (where n is the number of carbon atoms), results are given for the virial coefficients B_2, B_3, and B_4; results for B_5 are given for chains up to length $n=12$; and results for B_6 are given for chains of length $n=2$, 3, and 4. In all cases, values are given for temperatures ranging from 200 K to 2000 K in 20–50 K increments. The values are used to calculate the equation of state for butane and the pressure-density behavior is compared to experimental data at 350 and 550 K. Critical points are calculated for all systems and compared to simulation data previously taken for the same molecular model, and to experiment. The comparison with temperature is very good (within 1.5% for all chain lengths up to $n=12$), while the critical density is underestimated by about 5%–15% and the critical pressure is given within about 10%. The convergence behavior of the virial equation of state as applied across the n-alkane series is well characterized by corresponding states, meaning that the accuracy at a given density relative to the critical density does not deteriorate with increasing chain length. © *2010 American Institute of Physics*. [doi:10.1063/1.3486085]

I. INTRODUCTION

Modeling of chain molecules is a topic of longstanding interest, and while methods are becoming increasingly atomistic in nature, thermodynamic models still rely on highly idealized treatments of the inter- and intra-atomic interactions. In contrast, molecular simulations can accommodate highly detailed models, so they need not invoke severe approximations in the descriptions of the interactions. The price paid for this capability is a loss of analyticity; instead of an equation of state, molecular simulation yields a collection of data. Models can be fit to the data, of course, but this approach is not as clean as an equation of state formulated on a well-defined, albeit idealized molecular model.

The virial equation of state (VEOS) provides a compromise between thermodynamic models and molecular simulations.[1] The VEOS is a density expansion written with respect to an ideal-gas reference, and is written as follows:

$$\beta P = \rho + B_2\rho^2 + B_3\rho^3 + B_4\rho^4 + \cdots, \tag{1}$$

where P and ρ are the pressure and number density, respectively, $\beta=1/kT$ with T, the absolute temperature and k, Boltzmann's constant, and B_i is the ith virial coefficient, which is independent of density. We will denote as VEOSi the VEOS when truncated so that the highest order term that is included is B_i. Unlike parameters for traditional engineering models, the virial coefficients appearing in the VEOS have a rigorous connection to the molecular interactions. Interactions among only a few molecules at a time are needed, so the VEOS can potentially be applied to even more realistic models than typically used in molecular simulation. Of course, it suffers also from the significant limitation that it is valid only at low density, but the question of how low the density must be for the virial equation to be relevant has not been addressed in a comprehensive way. This is largely due to the difficulty of calculating high-order virial coefficients, which require evaluation of many-dimensional integrals over translational, rotational, and internal degrees of freedom of i molecules for the coefficient B_i. For this reason there are very few results for virial coefficients for chain molecules beyond B_2.[2] A notable exception is the work of Vega,[3] who examined hard-sphere chains, computing coefficients up to B_4 for chain lengths of as much as 100 using an approach in which the different conformations of the chains are viewed as different components of a mixture. The advent of the Mayer-sampling Monte Carlo method[4] has enabled the calculation of coefficients up to at least B_5 for multiatomic molecules[5,6] without much difficulty, including those that are not based on purely repulsive potentials, so we are positioned to investigate the applicability of the VEOS for a broader range of systems.

In the present work, we examine application to chain molecules. We examine in particular the virial coefficients for model n-alkanes up to C_{20}. Our calculations are based on the TraPPE-UA model,[7] which has been formulated to describe vapor-liquid coexistence well, and thus it aims to provide a good model for the gas phase. We consider how the coefficients and the convergence behavior of the VEOS vary with chain length, and we are particularly interested in the ability of the VEOS to identify the location of the critical point.

In Sec. II, we describe the models and briefly review the methods used to calculate the virial coefficients. Then in Sec. III we present and discuss results before concluding in Sec. IV.

[a]Electronic mail: ajs42@buffalo.edu.
[b]Tel.: 716-645-1173. FAX: 716-645-3822. Electronic mail: kofke@buffalo.edu.

II. MODELS AND METHODS

A. Model

All of our calculations are based on the TraPPE-UA model parameters for alkanes.[7] The model employs a united-atom (no explicit hydrogens) representation of the alkyl segments, which are modeled with a Lennard-Jones potential describing nonbonded interactions. Internal degrees of freedom include bond bending described by a harmonic bond-bending potential, and torsion with an associated dihedral potential. Fixed bond lengths are enforced for neighboring segments, so no bond stretching is permitted.

B. Evaluation of virial coefficients

The virial coefficients are given in terms of cluster integrals involving interactions among i molecules for the coefficient B_i. The classical second virial coefficient is

$$B_2(T) = -\frac{1}{2V\Omega^2}\int\int f_{12}e^{-\beta U_1}e^{-\beta U_2}d\mathbf{r}_1 d\mathbf{r}_2 d\boldsymbol{\omega}_1 d\boldsymbol{\omega}_2. \quad (2)$$

The integral is performed over all positions $\mathbf{r}_1$ and $\mathbf{r}_2$ in a volume V, which is taken to be infinite. In practice, we effect the division by V by holding the position of molecule 1 fixed. The symbols $\boldsymbol{\omega}_1$ and $\boldsymbol{\omega}_2$ represent all orientational and internal (conformation) coordinates of molecules 1 and 2, respectively, and $U_i(\boldsymbol{\omega}_i)$ is the intramolecular energy for molecule i. The integrals over $\boldsymbol{\omega}$ are normalized by dividing by $\Omega \equiv \int e^{-\beta U(\boldsymbol{\omega})}d\boldsymbol{\omega}$. Also, $f_{12}=\exp(-\beta u(\mathbf{r}_1,\mathbf{r}_2,\boldsymbol{\omega}_1,\boldsymbol{\omega}_2))$ is the Mayer function, where u is the total intermolecular energy between molecules 1 and 2. Expressions for higher order coefficients B_i involve sums of integrals over i molecules with the number of integrals growing rapidly with i.[8] For nonrigid molecules having intramolecular degrees of freedom—which includes molecules of interest here—additional contributions arise in the expressions for the virial coefficients B_3 and higher.[9] These contributions result, for example, from the fact that the interactions of one molecule with a second will affect the distribution of conformations adopted by the latter, which in turn influences its interactions with a third molecule. The result is that this chain of interactions cannot be decomposed into separate 1-2 and 2-3 integrations, precluding a cancellation with products of such two-body integrals, a cancellation that does occur for rigid molecules.

Mayer-sampling Monte Carlo (MSMC) (Ref. 4) is a general approach to calculation of the cluster integrals in which the configurations of the molecules are sampled according to a Markov process, much as is done in a standard Metropolis Monte Carlo (MC) simulation.[10] Previous applications have focused on monatomic molecules[4] and rigid multiatomics,[5] but the method is equally well applied to flexible molecules,[6] particularly the chain molecules of interest here. The sampling is performed of all molecular coordinates represented in the integrals above. Configurations are weighted according to the absolute value of the Mayer-function integrand $f_{12}e^{-\beta U_1}e^{-\beta U_2}$, or sum of integrands for coefficients B_i, $i>3$ that are given in terms of more than one cluster integral. The integrals are calculated using ideas derived from methods used to compute the free energy.[11] In most cases, we employ overlap sampling with Bennett's optimization,[12] for which the working equation in MSMC becomes[5,13]

$$\Gamma(T) = \Gamma_0 \frac{\langle \gamma/\pi\rangle_\pi / \langle \gamma_{OS}/\pi\rangle_\pi}{\langle \gamma_0/\pi_0\rangle_{\pi_0} / \langle \gamma_{OS}/\pi_0\rangle_{\pi_0}}. \quad (3)$$

Here we use Γ to represent a general cluster integral or virial coefficient, γ is the corresponding integrand (or sum of integrands) needed for its calculation, π is the function used to weight the sampling of configurations. The subscript 0 indicates a value for a known reference system, distinguishing it from the target system, which is absent a subscript. The angle brackets specify an ensemble average weighted by π or π_0. Also γ_{OS} is the overlap function, given in terms of the target and reference integrands as

$$\gamma_{OS} = \frac{|\gamma_0||\gamma|}{\alpha|\gamma_0| + |\gamma|}, \quad (4)$$

where α is a parameter selected to optimize the convergence of the calculation. Additionally, the distribution of computational effort expended between sampling the π and π_0 systems is balanced to ensure that their marginal contribution to the stochastic error of the result is equalized. As a reference system, we use monatomic hard spheres of diameter equal to (in angstrom) $\sigma_{HS}=\sigma_{CH_3}+0.5n_C$, where $\sigma_{CH_3}=3.75$ Å is the diameter of a TRaPPE-UA methyl group and n_C is the number of carbon atoms in the chain. The reference integrand γ_0 is the same function as γ but with the hard-sphere potential, and the sampling weights are just the absolute values of the integrand: $\pi=|\gamma|$, $\pi_0=|\gamma_0|$. When calculating the reference integrand, γ_0, we represent the molecules as hard spheres centered at the molecule's geometric center. Calculation of terms arising from molecular flexibility requires a variation on the MSMC method, but largely the approach is the same. We will report details of this procedure in a future publication.

C. Simulation details

MSMC simulations are performed in an infinite volume with no periodic boundaries and no truncation of the potential. One molecule is fixed at the origin, and the vanishing of π at large separations ensures that none of the molecules stray too far from it. It is worth remembering that in MSMC simulations, the weighting function does not prohibit sampling of configurations in which there is overlap of the repulsive cores of atoms on different molecules. Thus there is no steric hindrance to sampling. Some representative configurations observed during MSMC simulations are shown in Fig. 1.

The MSMC simulations included several types of MC moves to sample configurations. All simulations included moves that would translate any one of the molecules except the first (which is fixed at the origin). All simulations also included rotation moves, which were applied to a molecule selected at random (including the first molecule). Simulations of C_3 and higher included a move that selects a random atom from a molecule and moves it while keeping the bond lengths fixed. For simulations of C_4 and higher, we included

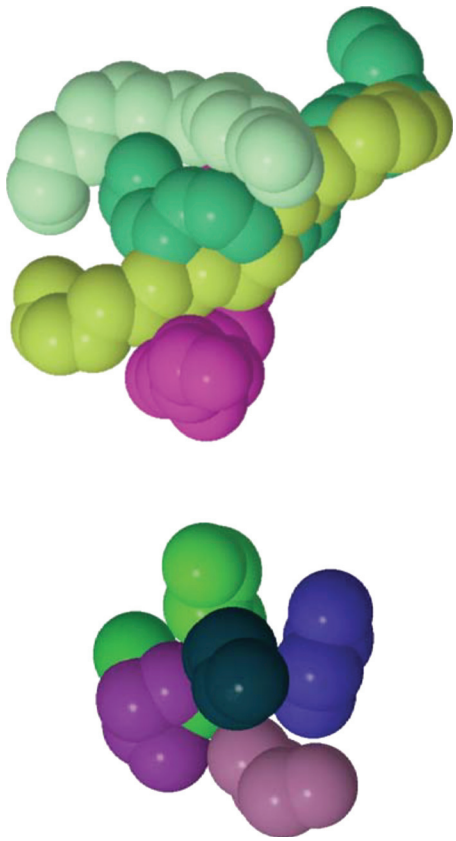

FIG. 1. Representative configurations from Mayer-sampling Monte Carlo simulations. On the bottom is shown a configuration from the calculation of B_6 for C_4 (butane), and on the top is a configuration from calculation of B_4 for C_{20}. Molecules are colored differently only to make them more distinguishable in the figure.

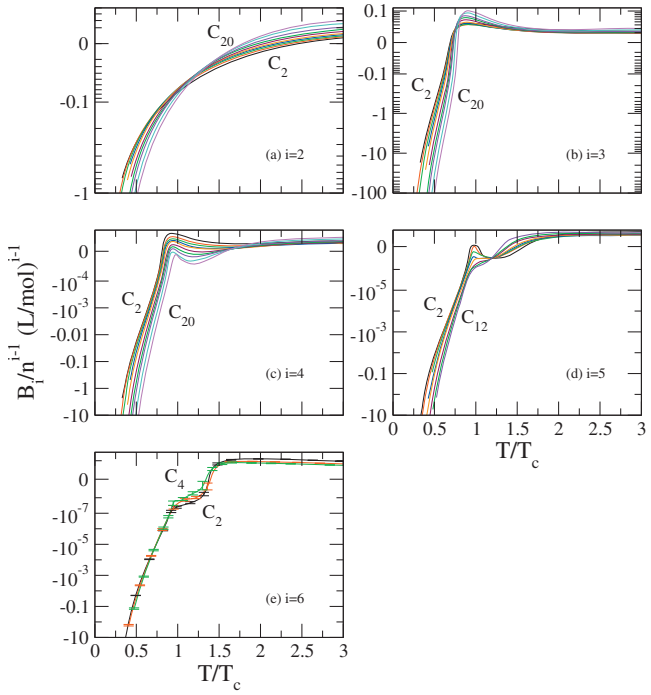

FIG. 2. Virial coefficients computed in this study, excluding the contributions from molecular flexibility. Temperature is scaled by literature values (Ref. 7) (or best estimate) of the critical temperature for the model, and virial coefficients B_i are scaled by the chain length n as indicated, and are plotted on an arcsinh scale. Curves proceed in sequence from C_2 to the largest n computed, as indicated on each plot. Confidence limits are smaller than the line thickness, except where shown.

another move that selects a torsion bond and rotates the molecule about it. The two parts of the molecule on either side of the torsion bond are rotated by $\phi/2$ and $-\phi/2$, respectively, where ϕ is the desired overall rotation angle. The new bond angle is selected from a Boltzmann distribution (determined numerically) for the torsion potential, allowing the simulation to quickly sample *trans* and *gauche* conformations.

The total amount of sampling performed varied considerably with chain length and order of the coefficient being computed. At least five independent calculations were performed for each case, and the quoted confidence limits are based on the standard error of the mean of the independent runs. Each such simulation sampled at least 10^8 configurations, including an equilibration phase that occupied 7.5% of the total run.

Calculation of molecular-flexibility contributions were completed for most but not all of the virial-coefficient/alkane combinations. In particular, we did not attempt calculation of these contributions to B_5 for chains longer than C_5, and we performed calculation of no such contributions to B_6 for any of the alkane models. The molecular-flexibility contributions were not determined with the same precision as the usual virial coefficient terms due to the relatively high cost of computing the additional contributions, and most values were moreover statistically zero. Their main effect in the systems studied here is to significantly reduce the precision we are able to report for the full virial coefficients, without significantly changing the computed values of the coefficients themselves. We report data both with and without these contributions.

III. RESULTS AND DISCUSSION

We calculated coefficients B_2, B_3, and B_4 for alkanes up to C_{20} (we indicate the normal alkane species by referencing just the number of carbons); we further calculated B_5 for alkanes up to C_8 and B_6 up to C_4. Values were computed for temperatures ranging from 200 K (sometimes lower) to 2000 K (sometimes higher) in 20–50 K increments. The upper range of temperature exceeds the decomposition temperature of real alkanes, but this is not an issue for the calculations.

All coefficients are presented as a function of temperature in Fig. 2, and the data are tabulated in files that are given in the supplementary material.[14] The results presented in Fig. 2 are scaled to highlight the similarity of the curves for different alkane lengths n. The temperature is scaled by the critical temperature of the model alkane (as determined from the data of Martin and Siepmann,[7] extrapolated as a function of $1/n$ if needed), and the virial coefficient B_i is scaled by the alkane chain length n raised to the $i-1$ power. Given that the critical mass density is found to be insensitive to chain length, this scaling has an effect similar to scaling by the critical molar density. The scaling is effective in putting the virial coefficients for different alkanes into the same frame, but significant differences do remain, showing the limits of this corresponding-states presentation. The figure shows the virial coefficients including only the biconnected-diagram

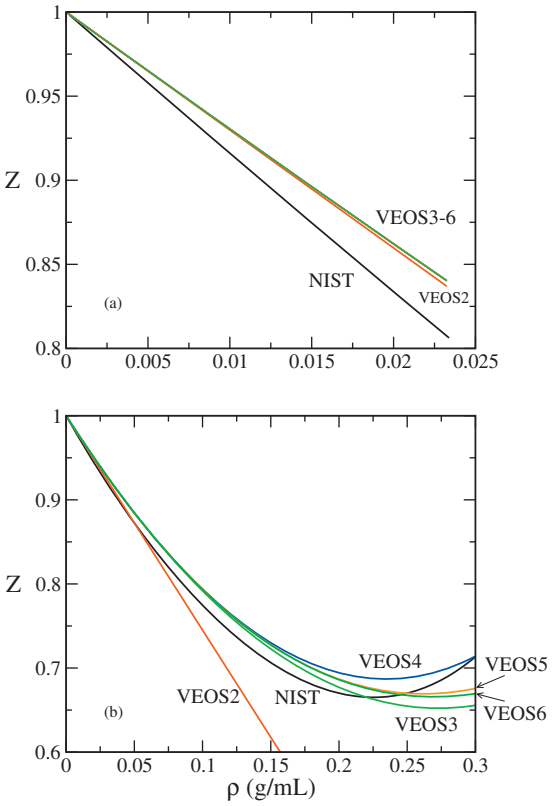

FIG. 3. Compressibility factor, $Z=P/\rho kT$ as a function of density, for butane at (a) 350 K and (b) 550 K, comparing the virial equation truncated at various orders as indicated to an accurate empirical correlation (Ref. 20).

contributions, without any corrections for molecular flexibility. We find that in only very few cases are such contributions significant (being both statistically different from zero, and larger than the confidence limits on the biconnected-diagram value). In particular for B_3, they contribute 5% of the total value for C_{20} at low to moderate temperatures, and less for shorter chains. For B_4 and B_5, the value of the corrections cannot be distinguished from zero statistically. Thus introducing them in Fig. 2 would largely have the effect of adding noise to the curves, making it difficult to perceive the overall trends.

In Fig. 3, we demonstrate the convergence behavior of VEOS (with coefficients including the molecular-flexibility contribution) while comparing to the experimental data, by selecting butane for this example. Two temperatures are shown, one subcritical with density plotted up to saturation, and one supercritical with density plotted up to about 30% above the critical density. For the subcritical case, the VEOS converges quickly, although the equation of state differs somewhat from experiment. The deviation is present over the whole density range, and indicates inaccuracy in B_2. Martin and Siepmann[7] computed B_2 for some of their alkane models and compared them to experiment, and this limit of the TraPPE-UA model has already been examined and discussed by them. The shortcoming represents a compromise required for a nonpolarizable model to describe vapor-liquid coexistence behavior. The comparison at supercritical conditions, which extends to a much higher density than the subcritical case, shows the progress toward convergence of VEOS with

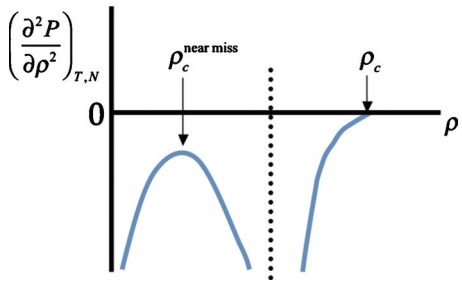

FIG. 4. Schematic illustration of the behavior of the second-derivative critical criterion following temperature-density lines for which the spinodal condition is satisfied (zero first derivative).

VEOS6 apparently providing an accurate description of the alkane model's behavior over the whole range of density shown. In comparison to experiment, the inaccuracy of B_2 is harder to detect and accordingly, it is less significant overall. Given the inherent limitation in reproducing B_2, the TraPPE-UA model is not so bad in capturing the larger behavior, which is consistent with its formulation as an effective two-body potential. The compromise that permits it to capture adequately both low- and medium-density behavior is evident in the figure.

The critical point for a pure substance is given from the equation of state by the conditions[15]

$$\left(\frac{\partial P}{\partial \rho}\right)_{T,N} = 0; \quad \left(\frac{\partial^2 P}{\partial \rho^2}\right)_{T,N} = 0; \quad \left(\frac{\partial^3 P}{\partial \rho^3}\right)_{T,N} \geq 0. \tag{5}$$

We apply the VEOS (with molecular-flexibility corrections included, when known) to determine the temperature and density at which the first two equations are satisfied, with the temperature dependence evaluated via interpolation of the tabulated virial coefficients.[16]

As we noted in our study of Lennard-Jones mixtures,[17] there are some isolated cases in which the criteria for criticality are not satisfied for any temperature or density when evaluated using VEOS truncated at some order. In such cases, we can identify conditions at which the criteria are most nearly satisfied, and in our experience, these values provide a meaningful estimate of the critical point. The situation is shown schematically in Fig. 4. The line shown there describes the behavior of the second derivative $\partial^2 P/\partial \rho^2$ when plotted at conditions of temperature and density for which the first derivative is zero, $\partial P/\partial \rho = 0$. Two cases are shown. In one case, we find a point at which $\partial^2 P/\partial \rho^2$ is zero, so a true critical point is indicated. In the other case, there is no point for which $\partial^2 P/\partial \rho^2$ is zero, so no critical point is indicated. Instead, we use the location of the maximum as a "near-miss" critical point. In this study, we encountered a near-miss critical point for only two instances, specifically VEOS5 for C_{10} and C_{12}.

We calculate the confidence limits on the critical points using a Monte Carlo process in which we perturb the virial coefficients by sampling from a Gaussian with standard deviation equal to the standard error of the mean. We do this for all the virial coefficients appearing in VEOS*i* and recalculate the critical properties each time. This is repeated 40 times and the collection of results for each critical property

are subjected to the usual error analysis to generate their confidence limits. In a small number of instances, the perturbed set of coefficients would no longer yield a critical point even though a critical point is found for the nominal set of coefficient values. This situation arose in the following cases: C_2/VEOS6, 5% of the perturbed coefficients produced only a near-miss critical; 15% for C_3/VEOS6; 7.5% for C_4/VEOS6; and 7.5% for C_8/VEOS5. These near-miss cases were discarded and not used for the error estimation. We also point out that the perturbation process a few times produced coefficients for which VEOS yielded a critical point even though the nominal coefficients found only the near-miss case. Thus for VEOS5 for C_{10}, 27.5% of the perturbed coefficients found a critical point, while 15% did for C_{12}. For the first case, the near-miss critical point differed from the perturbed-B_i critical temperature by about 1%, which is larger than the confidence limits themselves. The unsurprising point taken from this is that use of the near-miss critical point introduces some small inaccuracy that is nonetheless larger than any noise in the values.

The critical properties computed in this way are presented in Fig. 5 and in Table I, where they are compared to established values determined from molecular simulation, as well as experimental values for real alkanes. The comparison is similar to what we observed in applications to the monatomic Lennard-Jones model. The critical temperature is described surprisingly well, all the way up to C_{12}, which is the longest chain for which simulation data are available, and even to C_{20} considering just the comparison to experiment. The critical pressure shows a good agreement also, although some differences from the simulation values are noticeable (the remarkable agreement of VEOS4 for C_{16} and C_{20} is impressive, but no doubt fortuitous given the agreement of VEOS5 with simulation at C_{12}). The critical density agrees much less well with the literature, which we consider to be related to the nonclassical behavior of the equation of state near the critical point.[18]

The convergence of VEOS is examined in Fig. 6. Here we present a map in the temperature-density plane with lines demarcating regions of validity of VEOS to various orders. Specifically, for the line indicated VEOSi, we compute the "remainder" sum $r_i=\Sigma_{k=i+1}^{7}|B_k|\rho^k$ (note the absolute value) as well as the full sum $s=\Sigma_{k=1}^{7}|B_k|\rho^k$ (where $B_1=1$); for all points to the left of a given line, the remainder is less than 1% of the full sum. We interpret the line VEOSi as indicating where the next coefficient B_{i+1} starts to have a significant contribution to the total pressure, so all points to the left of it are well described by VEOS to the indicated order. Data are presented for C_1, C_2, C_4, and C_8 (the data for C_1 are the same as given in Ref. 13 for the Lennard-Jones model, with size and energy parameters chosen to model methane), with all values reduced by the corresponding critical properties. The anomalous rightward-oriented peaks occur where one of the coefficients in s (typically the first one in the sum) goes through zero.

The plots show a remarkable consistency of the convergence behavior for the different substances, when viewed in the corresponding-states framework obtained upon scaling by the critical properties.[15] This is a bit surprising, considering that longer-chain molecules are capable of interacting with more molecules at once, and thus one might expect higher-order coefficients to be more important. Offsetting this perhaps is the fact that the critical densities (when expressed in moles, not mass) decrease with chain length. So if expressed in terms of absolute molar densities—appropriate in the context of counting intermolecular interactions—the convergence region does shrink with increasing chain length for a given VEOSi. Nevertheless fluid behavior is most appropriately gauged in the context of vapor-liquid coexistence, and criticality. In this regard we see that VEOS, applied to modest order in density, is capable of reaching the vapor-phase spinodal density at all temperatures, and does indeed (as seen in the comparisons above) encompass the critical region (notwithstanding effects of nonclassical scaling). Even higher densities are obtainable for temperatures beyond the scale of the figure, particularly for the higher-order VEOS; but the upper limit of the plot is already well above the decomposition temperature of the alkanes, so we do not present this extension.

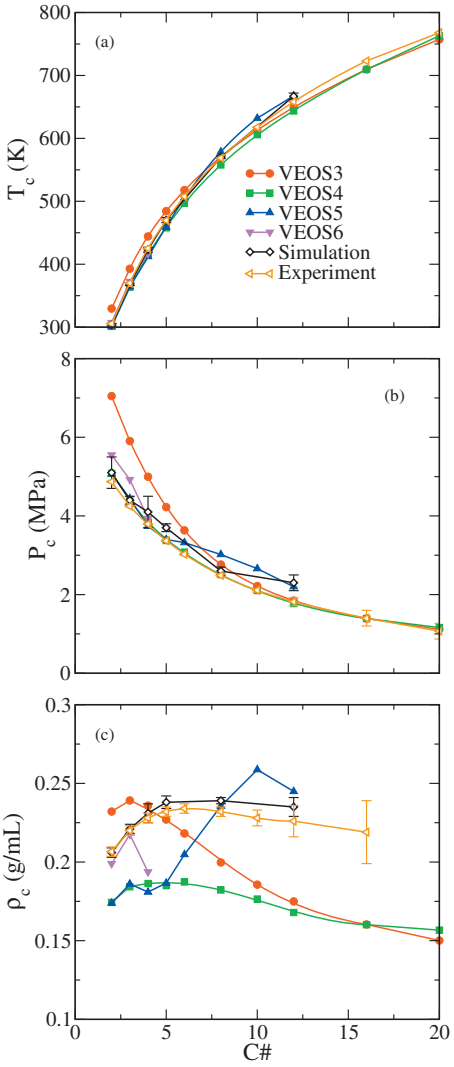

FIG. 5. Critical properties as given by the VEOS to various orders as a function of n-alkane carbon number. Results are compared to values obtained by Monte Carlo simulation applied to evaluate the critical points for the same model (Ref. 7) and to the experimental data for real alkanes (Ref. 19). Error bars are indicated only when larger than the symbol size. Lines join points as a guide to the eyes.

TABLE I. Critical properties as given by VEOS*n* for the model alkanes examined in this study.

n	T_c (K)	P_c (MPa)	ρ_c (g/ml)
		C_2	
3	329.46(3)	7.0472(13)	0.232 07(3)
4	301.19(9)	5.081(5)	0.174 33(15)
5	301.0(2)	5.069(13)	0.1739(4)
6	307.4(12)	5.55(10)	0.199(8)
Sim[a]	304(2)	5.1(4)	0.206(3)
Expt.[b]	305.32(4)	4.872(10)	0.2066(30)
		C_3	
3	392.8(4)	5.904(9)	0.239 13(14)
4	363.4(3)	4.405(9)	0.1843(3)
5	364.2(10)	4.44(5)	0.186(2)
6	373(2)	4.92(15)	0.218(12)
Sim[a]	368(2)	4.4(1)	0.221(3)
Expt.[b]	369.83(10)	4.248(10)	0.220(3)
		C_4	
3	444.2(2)	4.996(5)	0.235 91(12)
4	415.0(5)	3.844(16)	0.1863(7)
5	412(3)	3.74(10)	0.181(5)
6	417(4)	3.94(19)	0.194(15)
Sim[a]	423(4)	4.1(4)	0.231(6)
Expt.[b]	425.12(10)	3.796(10)	0.228(3)
		C_5	
3	484.36(14)	4.223(4)	0.227 00(15)
4	457.9(11)	3.37(3)	0.1850(15)
5	459(3)	3.40(10)	0.187(7)
Sim[a]	470(4)	3.7(1)	0.238(4)
Expt.[b]	469.7(2)	3.370(20)	0.232(3)
		C_6	
3	517.8(3)	3.633(7)	0.2182(3)
4	497.3(17)	3.08(4)	0.187(2)
5	506(3)	3.32(8)	0.205(5)
Expt.[b]	507.6(2)	3.025(20)	0.234(3)
		C_8	
3	570.2(6)	2.763(8)	0.1998(4)
4	558(3)	2.51(5)	0.182(4)
5	578(4)	3.02(10)	0.236(12)
Sim[a]	570(2)	2.6(1)	0.239(2)
Expt.[b]	568.7(3)	2.49(3)	0.232(3)
		C_{10}	
3	613.1(6)	2.217(8)	0.1856(5)
4	606(3)	2.10(5)	0.176(4)
5[c]	632(4)	2.66(9)	0.259(18)
Expt.[b]	617.7(6)	2.11(5)	0.228(5)
		C_{12}	
3	649.3(4)	1.848(5)	0.1750(3)
4	643(4)	1.77(5)	0.168(4)
5[c]	668(4)	2.20(6)	0.245(12)
Sim[a]	667(5)	2.3(2)	0.235(6)
Expt.[b]	658(1)	1.82(10)	0.226(10)
		C_{16}	
3	709.6(14)	1.392(11)	0.1603(9)
4	710(11)	1.39(11)	0.160(12)
Expt.[b]	723(2)	1.40(20)	0.219(20)
		C_{20}	
3	757(2)	1.115(12)	0.1501(12)
4	763(12)	1.16(11)	0.157(18)
Expt.[b]	768(8)	1.07(20)	

[a]Results from molecular simulations performed on the same model (Ref. 7).
[b]Experimental values (Ref. 19).
[c]Near-miss critical point.

IV. CONCLUDING REMARKS

An appealing feature of the VEOS as applied in conjunction with MSMC is the ease to which it is extended to the multiatomic system. The VEOS is formulated at the level of molecules, not atoms, and much of the complexity that accompanies the extension of many statistical mechanical theories to multiatomics does not arise when working with VEOS. The contributions related to molecular flexibility are a bit troublesome to obtain precisely, but the complications accompanying their calculation are not great, and moreover the difficulty of implementing the calculation is not affected by size or structure of the molecules. Otherwise, the primary accommodation that must be made for multiatomics is the added sampling of rotational and conformational degrees of freedom in the MSMC simulations. This however is a trivial burden and no real obstacle to application of the methods to such systems. It is also notable that we require no evaluation of single-molecule conformational partition functions [Ω in Eq. (2)], which sometimes arise in other treatments of fluids. These terms cancel when forming the ensemble-average ratios appearing in the MSMC approach. This more than anything is a consequence of the focus on the equation of state;

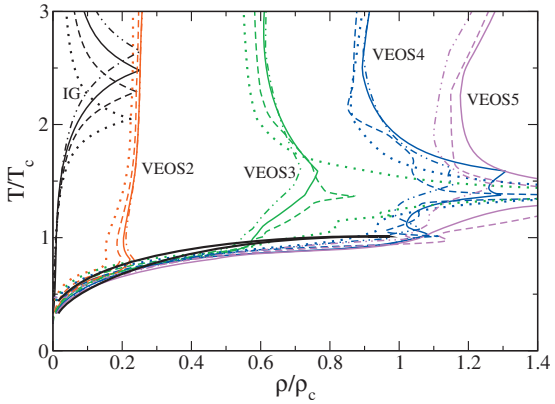

FIG. 6. Lines showing for four model alkanes approximate upper limits of applicability of the ideal-gas (IG) model and the virial equation to various orders (VEOS*i*). Dash-dotted lines: methane (Ref. 13); solid lines: ethane; dashed lines: butane; and dotted lines: octane. Thick black lines ending at the critical point are spinodals for C_2 from VEOS6 (right-most curve) and C_8 from VEOS4 (left-most curve). Temperatures and densities are reduced by critical values for the same model (Ref. 7).

if one is interested in using the VEOS to evaluate internal energies or free energies, then single-molecule averages must be treated as well.

Our previous work examining the VEOS in application to the monatomic Lennard-Jones model found that, if applied at sufficiently high order in density, it could accurately describe the pressure-density-temperature behavior over much of the state space away from the condensed liquid, including the subcritical gas phase up to the spinodal, the critical region, and rather high densities for supercritical temperatures. The present study shows that this performance is not diminished when extended to multiatomic molecules, and that the overall convergence properties of VEOS for alkanes is well aligned with corresponding-states theory.

ACKNOWLEDGMENTS

This work is supported by the National Science Foundation Grant Nos. CHE-0626305 and CBET-0854340. Calculations were performed using resources from the University at Buffalo Center for Computational Research. We are grateful to Katherine Shaul for assistance with calculation of the molecular-flexibility contributions to the virial coefficients.

[1] E. A. Mason and T. H. Spurling, *The Virial Equation of State* (Pergamon, Oxford, 1969); A. J. Masters, J. Phys.: Condens. Matter **20**, 1 (2008).
[2] J. M. Wichert and C. K. Hall, Macromolecules **27**, 2744 (1994); Y. C. Chiew and V. Sabesan, Fluid Phase Equilib. **155**, 75 (1999); A. Yethiraj, K. Honnell, and C. Hall, Macromolecules **25**, 3979 (1992).
[3] C. Vega, Mol. Phys. **98**, 973 (2000); C. Vega, J. M. Labaig, L. G. MacDowell, and E. Sanz, J. Chem. Phys. **113**, 10398 (2000).
[4] J. K. Singh and D. A. Kofke, Phys. Rev. Lett. **92**, 220601 (2004).
[5] K. M. Benjamin, A. J. Schultz, and D. A. Kofke, Ind. Eng. Chem. Res. **45**, 5566 (2006); J. Phys. Chem. C **111**, 16021 (2007); J. Phys. Chem. Br. **113**, 7810 (2009); K. M. Benjamin, J. K. Singh, A. J. Schultz, and D. A. Kofke, J. Phys. Chem. B **111**, 11463 (2007).
[6] K. R. Shaul, A. J. Schultz, and D. A. Kofke, "Mayer-sampling Monte Carlo calculations of methanol virial coefficients," Mol. Simul. (in press).
[7] M. G. Martin and J. I. Siepmann, J. Phys. Chem. B **102**, 2569 (1998).
[8] J. P. Hansen and I. R. McDonald, *Theory of Simple Liquids*, 3rd ed. (Academic, London, 2006).
[9] S. Caracciolo, B. M. Mognetti, and A. Pelissetto, J. Chem. Phys. **125**, 094903 (2006); **125**, 094904 (2006).
[10] D. Frenkel and B. Smit, *Understanding Molecular Simulation: From Algorithms to Applications*, 2nd ed. (Academic, New York, 2002).
[11] D. A. Kofke, Mol. Phys. **102**, 405 (2004); Fluid Phase Equilib. **228–229**, 41 (2005); D. A. Kofke and D. Frenkel, in *Handbook of Molecular Modeling*, edited by S. Yip (Kluwer, Dordrecht, 2004).
[12] C. H. Bennett, J. Comput. Phys. **22**, 245 (1976).
[13] A. J. Schultz and D. A. Kofke, Mol. Phys. **107**, 2309 (2009).
[14] See supplementary material at http://dx.doi.org/10.1063/1.3486085 for values of all calculated virial coefficients.
[15] J. W. Tester and M. Modell, *Thermodynamics and Its Applications*, 3rd ed. (Prentice Hall PTR, Upper Saddle River, NJ, 1997).
[16] A. J. Schultz and D. A. Kofke, Mol. Phys. **107**, 1431 (2009).
[17] A. J. Schultz and D. A. Kofke, J. Chem. Phys. **130**, 224104 (2009).
[18] E. H. Chimowitz, *Introduction to Critical Phenomena in Fluids* (Oxford University Press, New York, 2005).
[19] D. Ambrose and C. Tsonopoulos, J. Chem. Eng. Data **40**, 531 (1995).
[20] H. Miyamoto and K. Watanabe, Int. J. Thermophys. **22**, 459 (2001).